

Support Information

Mechanisms in the Catalytic Reduction of N₂O by CO over the M₁₃@Cu₄₂ Clusters of Aromatic-Like Inorganic and Metal Compounds

Table of Contents

Figure S1. The initial and final structures of N₂O adsorption on Cu₅₅ cluster systems.

Figure S2. Potential energy profiles, the optimized intermediates and transition states for N₂O decomposition to N₂ on the Co₁₃@Cu₄₂ cluster.

Figure S3. Potential energy profiles, the optimized intermediates and transition states for N₂O decomposition to N₂ on the Zn₁₃@Cu₄₂ cluster.

Figure S4. Potential energy profiles, the optimized intermediates and transition states for N₂O decomposition to N₂ on the Ru₁₃@Cu₄₂ cluster.

Figure S5. Potential energy profiles, the optimized intermediates and transition states for N₂O decomposition to N₂ on the Rh₁₃@Cu₄₂ cluster.

Figure S6. Potential energy profiles, the optimized intermediates and transition states for N₂O decomposition to N₂ on the Pd₁₃@Cu₄₂ cluster.

Figure S7. Potential energy profiles, the optimized intermediates and transition states for N₂O decomposition to N₂ on the Pt₁₃@Cu₄₂ cluster.

Figure S8. Local density of states (LDOS) of M₁₃@Cu₄₂ clusters (M = Cu, Co, Ni, Zn, Ru, Rh, Pd, Pt).

Table S1. Adsorption energies of different adsorption modes (N, O) and different adsorption sites for N₂O on Cu₅₅ cluster (ΔE_{ads}), charge transfer between the molecule and cluster (CT).

Table S2. The molecular energies, Zero-point energy (ZPE), entropic corrections (TΔS) at T = 298.15 K to the free energies and (ZPE-TΔS) values of the gas-phase.

Table S3. The free energies of the adsorbed species at T = 298.15 K.

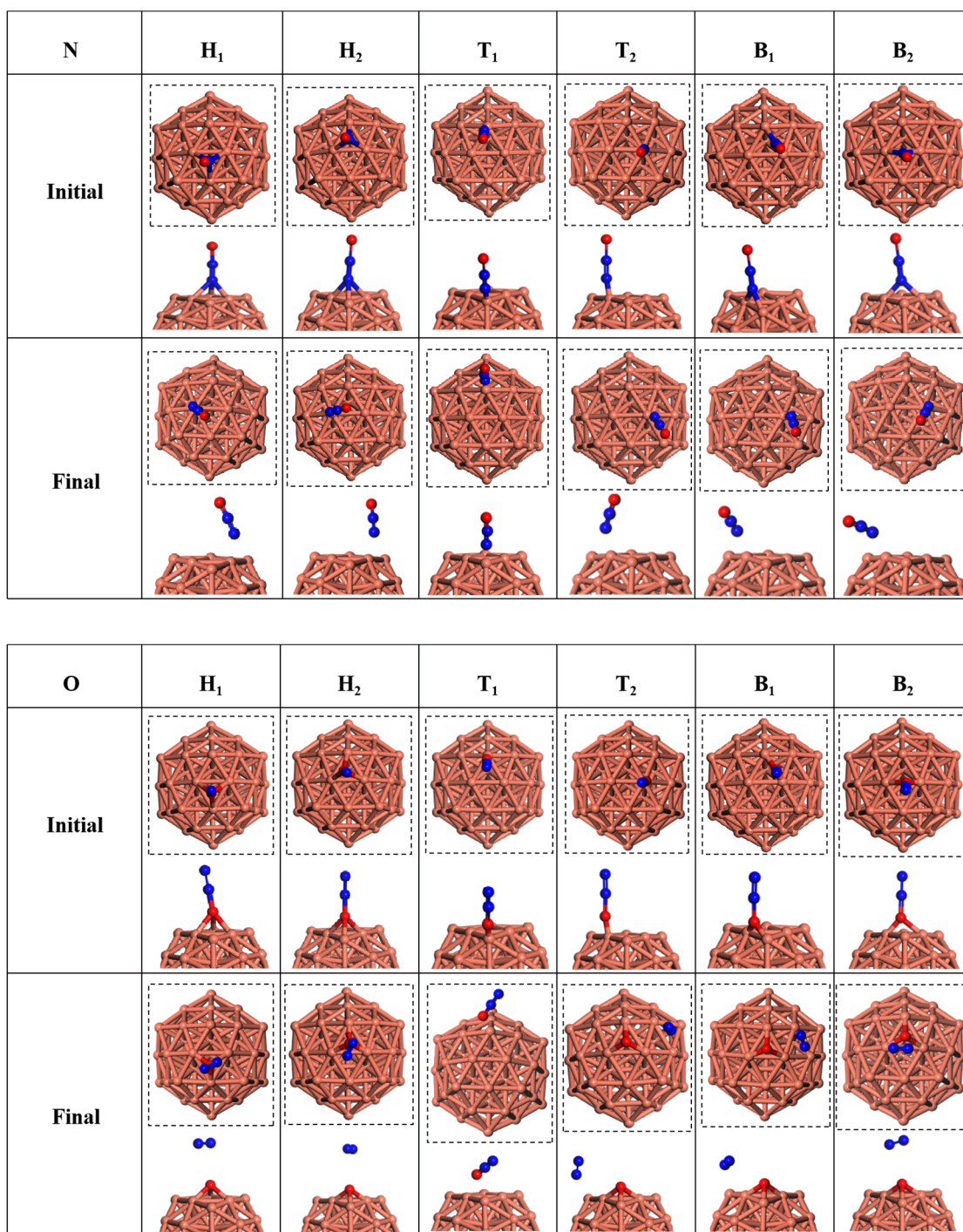


Figure S1. The initial and final structures of N₂O adsorption on Cu₅₅ cluster systems. The left superscript “N” or “O” indicates the N terminal or O terminal manners in N₂O adsorption.

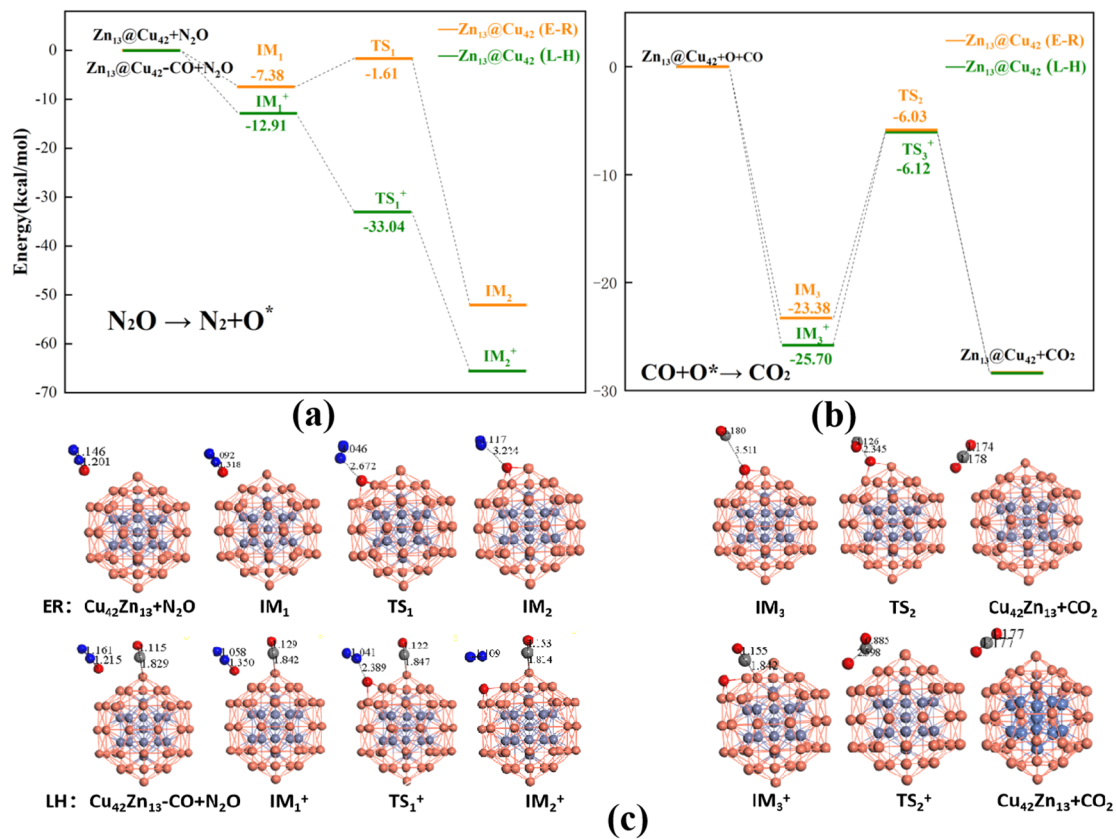


Figure S2. (a) and (b) Potential energy profiles for N_2O decomposition to N_2 on the $\text{Co}_{13}\text{@Cu}_{42}$ cluster. (c) Corresponding optimized intermediates and transition states involved in CO oxidation on the $\text{Co}_{13}\text{@Cu}_{42}$ cluster.

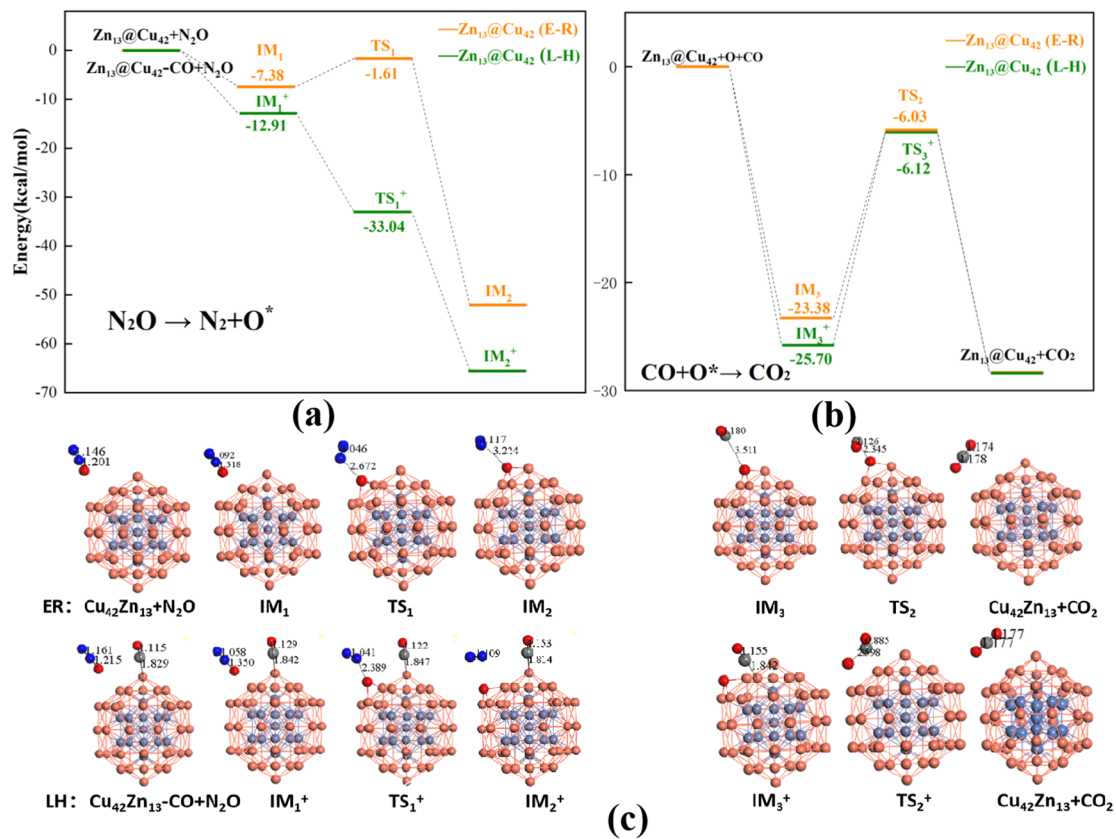


Figure S3. (a) and (b) Potential energy profiles for N_2O decomposition to N_2 on the $\text{Zn}_{13}\text{@Cu}_{42}$ cluster. (c) Corresponding optimized intermediates and transition states involved in CO oxidation on the $\text{Zn}_{13}\text{@Cu}_{42}$ cluster.

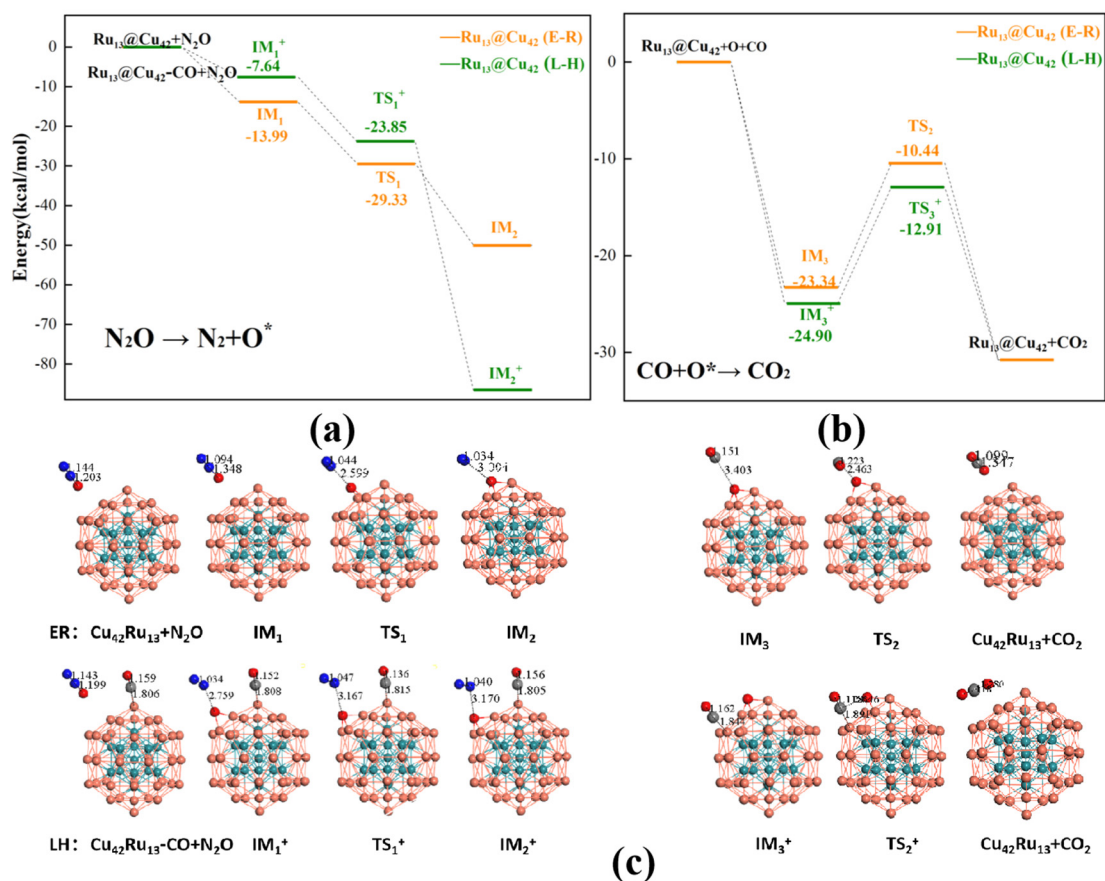


Figure S4. (a) and (b) Potential energy profiles for N_2O decomposition to N_2 on the $\text{Ru}_{13}@\text{Cu}_{42}$ cluster. (c) Corresponding optimized intermediates and transition states involved in CO oxidation on the $\text{Ru}_{13}@\text{Cu}_{42}$ cluster.

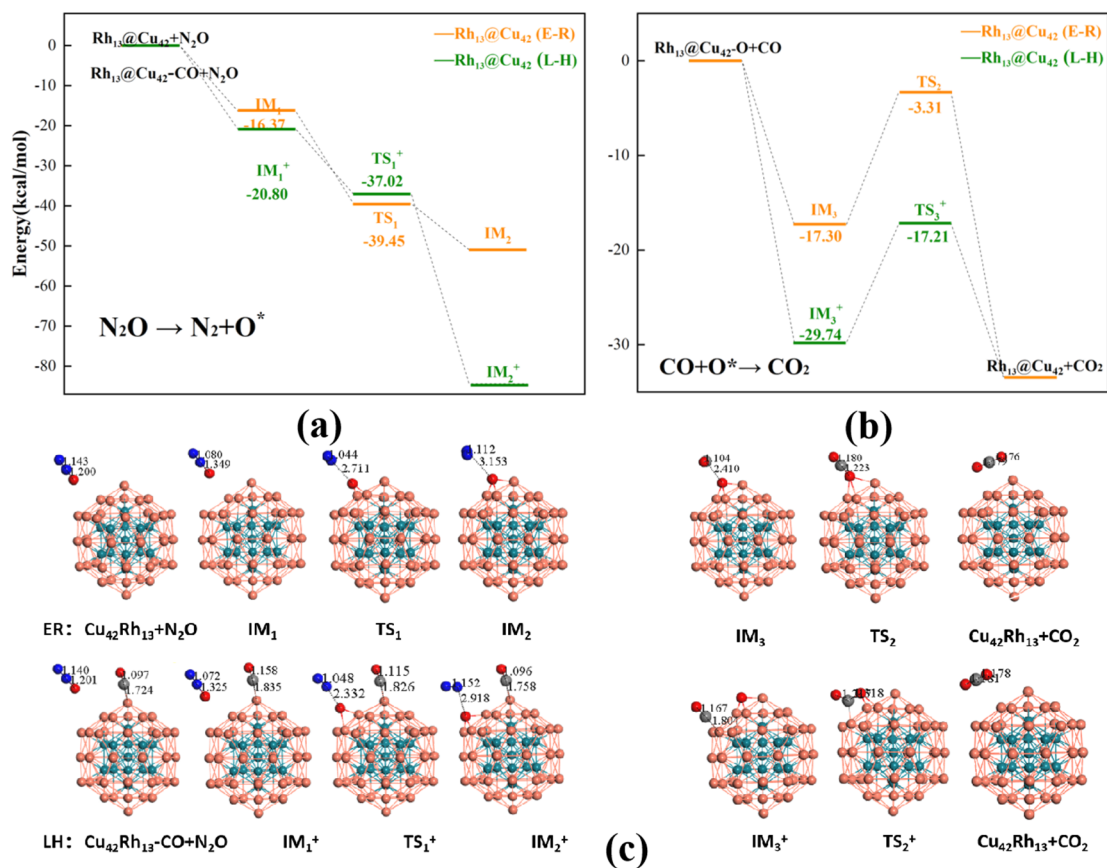


Figure S5. (a) and (b) Potential energy profiles for N_2O decomposition to N_2 on the $\text{Rh}_{13}@Cu_{42}$ cluster. (c) Corresponding optimized intermediates and transition states involved in CO oxidation on the $\text{Rh}_{13}@Cu_{42}$ cluster.

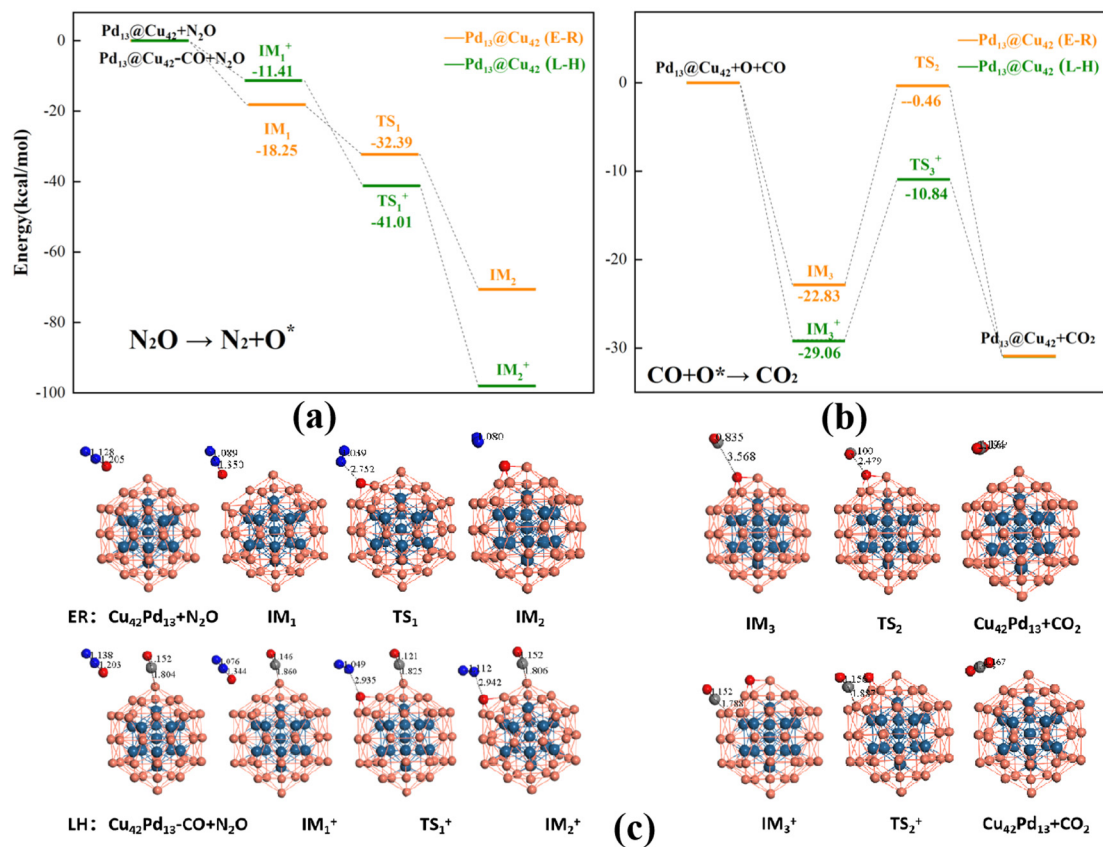


Figure S6. (a) and (b) Potential energy profiles for N_2O decomposition to N_2 on the $\text{Pd}_{13}@\text{Cu}_{42}$ cluster. (c) Corresponding optimized intermediates and transition states involved in CO oxidation on the $\text{Pd}_{13}@\text{Cu}_{42}$ cluster.

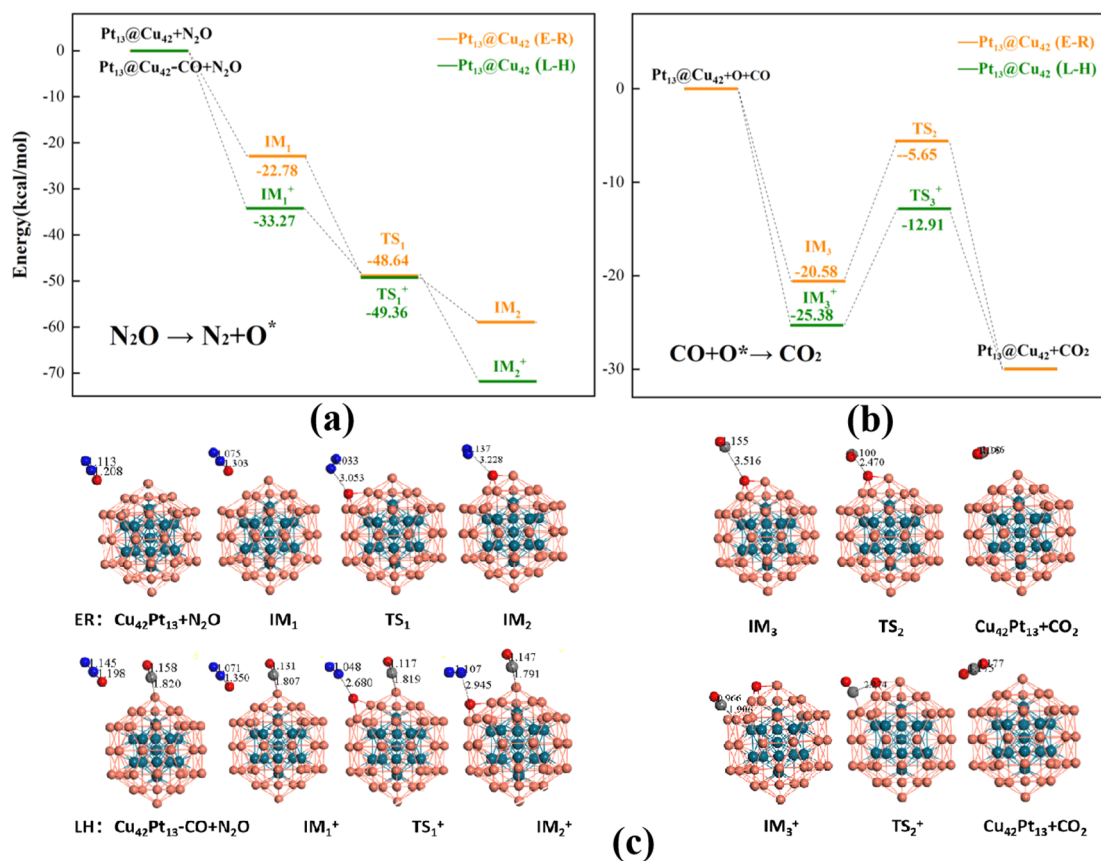


Figure S7. (a) and (b) Potential energy profiles for N_2O decomposition to N_2 on the $\text{Pt}_{13}@Cu_{42}$ cluster. (c) Corresponding optimized intermediates and transition states involved in CO oxidation on the $\text{Pt}_{13}@Cu_{42}$ cluster.

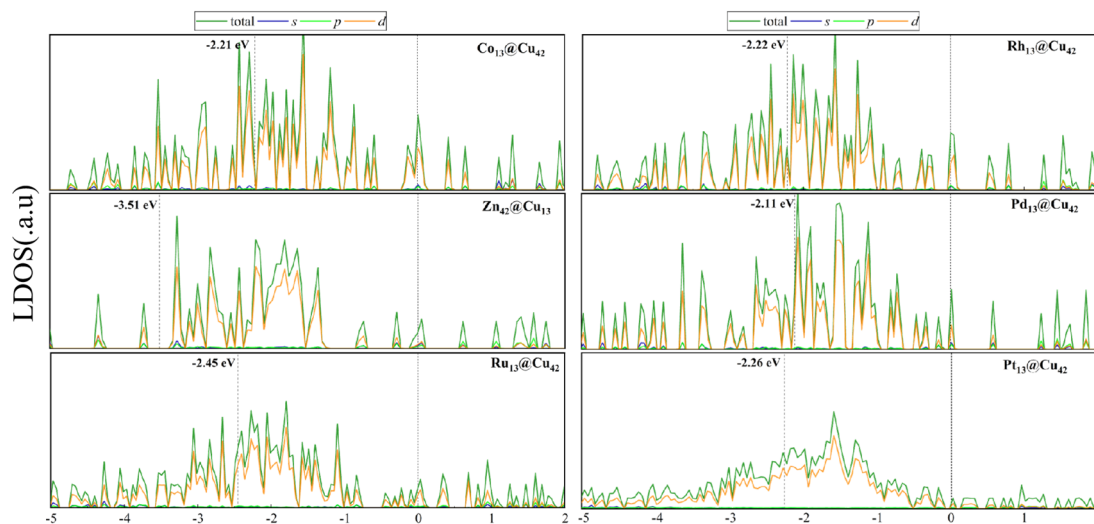


Figure S8. Local density of states (LDOS) of various $M_{13}@Cu_{42}$ clusters ($M = Cu, Co, Ni, Zn, Ru, Rh, Pd, Pt$). For each system, the HOMO level marked by the black dashed line is shifted to zero, and the red dashed lines and the numbers next to them indicate the d band center.

Table S1. Adsorption energies of different adsorption modes (N, O) and different adsorption sites for N₂O on Cu₅₅ cluster (ΔE_{ads}), charge transfer between the molecule and cluster (CT).

	Property	H ₁	H ₂	B ₁	B ₂	T ₁	T ₂
N	ΔE_{ads} (eV)	-7.38	-7.15	-7.61	-7.38	109.77	-7.38
	CT (e)	0.11	0.11	0.11	0.11	0.49	0.11
O	ΔE_{ads} (eV)	-48.43	-53.27	-53.27	-53.27	-3.46	-53.27
	CT (e)	0.96	0.97	0.97	0.97	0.03	0.97

Table S2. The molecular energies, Zero-point energy (ZPE), entropic corrections ($T\Delta S$) to the free energies and ($ZPE - T\Delta S$) values of the gas-phase. The Zero-point energy (ZPE) and entropic corrections ($T\Delta S$) at $T = 298.15$ K to the free energies values were taken from NIST-JANAF

thermodynamic table.

	N ₂	N ₂ O	CO	CO ₂
E (eV)	-383.49	-493.48	-340.83	-529.23
ΔG (eV)	-16.20	-20.95	-14.24	-22.61
ZPE (ev)	3.46	6.91	3.23	7.15
$T\Delta S$ (eV)	13.37	17.06	15.45	14.99

Table S3. The Gibbs free energies of the adsorbed species at $T = 298.15$ K. The Zero-point energy (ZPE) and entropic corrections ($T\Delta S$).

E-R	Cu	Co	Ni	Zn	Ru	Rh	Pd	Pt
ΔGN_2O (eV)	-52.12	-51.19	-47.04	-51.42	-50.96	-51.65	-71.49	-58.80
ΔGCO (eV)	-31.13	-32.28	-36.43	-32.05	-32.28	-31.59	-11.99	-24.44
L-H	Cu	Co	Ni	Zn	Ru	Rh	Pd	Pt
ΔGN_2O (eV)	-88.32	-93.16	-89.01	-92.70	-102.37	-100.31	-113.46	-90.16
ΔGCO (eV)	2.77	7.84	4.38	6.92	4.84	8.30	9.69	4.84